Journal of Power Sources 237 (2013) 19–25

Contents lists available at SciVerse ScienceDirect

Journal of Power Sources

journal homepage: www.elsevier.com/locate/jpowsour

Cell architecture upswing based on catalyst coated membrane (CCM) for vanadium flow battery

Chuan Yao [a,b], Huamin Zhang [a,*], Tao Liu [a], Xianfeng Li [a], Zonghao Liu [c]

[a] Division of Energy Storage, Dalian Institute of Chemical Physics, Chinese Academy of Sciences, Dalian 116023, China
[b] Graduate School of Chinese Academy of Sciences, Beijing 100039, China
[c] Dalian Rongke Power Co. Ltd., Dalian 116025, China

HIGHLIGHTS

- Power density of VFB is evidently improved by CCM architecture upswing.
- The energy efficiency of VFB reaches as high as 81.2% at 120 mA cm^{-2}
- The cell assembled with CCM exhibits excellent long-term cycle stability.
- CCM provides an effective way for electro-catalyst practical application in VFB.

ARTICLE INFO

Article history:
Received 24 September 2012
Received in revised form
26 February 2013
Accepted 4 March 2013
Available online 14 March 2013

Keywords:
Vanadium flow battery
Catalyst coated membrane
Electro-catalyst
Graphite felt
Efficiency

ABSTRACT

To promote the practical application of electro-catalyst in vanadium flow battery, cell architecture based on catalyst coated membrane (CCM) is designed. CCM is prepared via spraying electro-catalyst tungsten trioxide/super activated carbon, which exhibits excellent electrochemical performance toward vanadium redox couples, on both sides of the membrane. Results show that the use of CCM structure reduces the charge transfer impedance of the cell, and thus improves the energy efficiency and the power density remarkably. The voltage efficiency and energy efficiency reach as high as 85.9% and 81.2%, respectively, much higher than that using the traditional cell structure (81.3% and 76.9%) at 120 mA cm^{-2}. No loss in efficiency after 300 cycles indicates the favorable cycle stability of CCM. Therefore, CCM can be used as a promising vanadium flow battery structure for enhanced efficiency and power density.

1. Introduction

In recent years, the increasing demand of electrical energy and the limited supply of fossil fuel are incompatible. Therefore, large scale development and utilization of renewable energy such as solar and wind energy has become an urgent task in the face of human society. However, the instability and intermittence nature make these renewable sources difficult to meet the terminal demand. They must recur to a secure and effective energy storage system to smooth the energy supply [1]. Vanadium flow battery (VFB), first proposed by M. Skyllas-Kazacos in 1985 [2], is considered to be a promising technology for this application due to its high energy conversion efficiency, high reliability, long cycle life, flexible design, fast response, and low operation and maintenance costs [3–6]. It employs VO^{2+}/VO_2^+ and V^{2+}/V^{3+} redox couples as the positive and negative active species, respectively, with the standard open circuit cell voltage of approximate 1.26 V [2]. Using the same element at both electrodes offers the advantage of low cross-contamination between the positive and negative electrolytes [7]. Comprehensive social attention and scientific research are speeding up the progress of its commercialization.

Electrode is one of the key materials of VFB. Its physicochemical properties could strongly impact the energy conversion efficiency, the power density, and the energy density. The ordinary electrode materials are carbon felt (CF) or graphite felt (GF) with several millimeters thickness. The advantages of these materials are good stability in strong acid solutions and a relative large surface area [8]. However, the bare CF or GF still shows low electrochemical activity and poor kinetic reversibility [9]. Consequently, much attention has been paid to improve the electrochemical performance of the

* Corresponding author. Tel.: +86 411 84379072; fax: +86 411 84665057.
E-mail address: zhanghm@dicp.ac.cn (H. Zhang).

0378-7753/$ – see front matter © 2013 Elsevier B.V. All rights reserved.
http://dx.doi.org/10.1016/j.jpowsour.2013.03.014

electrodes. To this end, many researches are focused on the modification of CF or GF by thermal activation [10], sulfuric acid treatment [11] and electrochemical oxidation [9,12]. The main objective is to introduce oxygenated functional groups onto the fiber surface, to increase the active sites and improve the hydrophilicity of the fiber in the electrolyte. In recent years, it is found that depositing electro-catalyst such as metals (Ir, Bi) [13,14], alloys ($CuPt_3$) [15] and mental oxides (Mn_3O_4) [16] onto the fiber surface can greatly enhance the electrochemical performance of CF. However, the poor mechanical stability hampers their practical application [16]. Meanwhile, many novel carbon-based electro-catalysts with high activity are developed [17–19]. Shao et al. developed a nitrogen-doped mesoporous carbon (N-MPC) as the electrode material for the redox of VO^{2+}/VO_2^+. The electrochemical performance is significantly enhanced on N-MPC electrode than graphite electrode [18]. Han et al. reported the electrode material of graphene oxide nanoplatelets. It exhibits excellent electro-catalysis for VO^{2+}/VO_2^+ and V^{2+}/V^{3+} redox couples [19]. However, few reports were concerned on the practical application of these materials under VFB operating condition. Hence it is very necessary to find an effective way to make these highly active electro-catalysts for actual application.

Catalyst coated membrane (CCM) is one of the feasible methods for electro-catalyst practical application. It was widely used in direct methanol fuel cells (DMFCs) and proton exchange membrane fuel cells (PEMFCs) due to its high catalyst utilization and the establishment of the extended catalyst/membrane interface [20–22]. However, so far as we know, using CCM for VFB application has been rarely reported [23]. The electro-catalyst on the surface of CCM can form a compact layer when the binder existed. Compared with the catalyst loading on graphite felt fiber, the catalyst layer bears better mechanical stability, avoiding the problem of the electro-catalyst being brushed off in the flowing electrolyte. The catalyst layer, with excellent catalytic activity, could accelerate the kinetic progress of the electrode reactions, thus the voltage efficiency and energy efficiency of the cell can be improved.

In this paper, CCM was fabricated by spraying tungsten trioxide/super activated carbon (WO_3/SAC) electro-catalyst on both sides of Nafion115 ion exchange membrane. Cyclic voltammetry was employed to compare the electrochemical performance of WO_3/SAC electro-catalyst and the graphite material. Cell architectures based on CCM application were designed by two approaches. Single cell and AC impedance investigations demonstrated the effects of CCM introduction.

2. Experimental

2.1. CCM preparation

Electro-catalyst WO_3/SAC was prepared by impregnation method as described in our previous work [24]. Super activated carbon (SAC) with large surface area and low graphite degree (Jinzhou Changhong Petrochemical Co., Ltd, surface area: 2900 $m^2\ g^{-1}$, pore cubage: 1.588 mL g^{-1}) served as the support. The loading of WO_3 was 43.0 wt.%. Electro-catalyst ink was prepared by dispersing WO_3/SAC in isopropanol, ultra-sonicated for 30 min at ambient temperature to homogeneous dispersion. The ratio of electro-catalyst and solvent was 10 mg mL^{-1}. Proper Nafion solution (5 wt.%, Dupont Inc., USA, the mass ratio of WO_3/SAC and Nafion was 3:1) was added to the as prepared ink serving as the binder. Before CCM fabrication, Nafion 115 ion exchange membrane (Dupont Inc., USA, H^+ form) was cut into 5 cm × 5 cm and immerged in the deionized water for 24 h. A glass plate was cleaned by acetone and washed by deionized water several times. The membrane was took out and extended on the glass. The surface water was wiped off by filter paper. The edge of the membrane was fixed up on the glass plate surface by adhesive tape to expose an active area of 3 cm × 3 cm. Then, the as prepared catalyst ink was uniformly sprayed onto the membrane by a spray gun. According to the same steps above, the catalyst ink was also sprayed on the other side of the membrane.

2.2. Electrochemical tests of the graphite felt and the electro-catalyst WO_3/SAC

Before comparing the electrochemical performance of graphite felt with electro-catalyst WO_3/SAC powder, the graphite felt (Liaoyang Jingu Carbon Fiber Sci-Tech Co., Ltd., porosity: 91.2%, surface area: ~1 $m^2\ g^{-1}$) was firstly grinded to graphite powder. The morphology of graphite felt and the graphite powder were characterized by a scanning electron microscopy (SEM) (JEOL/EO, JCM-6000 Instrument, Japan). For preparing the working electrode, 10 mg WO_3/SAC or graphite powder and 50 μL Nafion solution (5wt.%) were added into 1 mL isopropanol, sonicated for 30 min to get fully dispersed ink. 20 μL of the as prepared ink was dripped on the surface of the glass carbon disk electrode (0.1256 cm^2) to form a thin film. Although there are some differences between the graphite felt and the graphite powder thin film, such as porosity and conductivity, the latter is still a good approximator of the former in electrochemical characterization. Cyclic voltammetry was conducted at ambient temperature on a workstation (CHI600b, CH Instruments, USA) using three-electrode system employing the electrode mentioned above as the working electrode, saturated calomel electrode (SCE) as the reference electrode, and large area graphite plate as the counter electrode. The investigations for VO^{2+}/VO_2^+ and V^{2+}/V^{3+} redox couples were carried out in 0.5 M $VOSO_4$ + 0.25 M $(VO_2)_2SO_4$ + 3.25 M H_2SO_4 and 0.5 M VSO_4 + 0.25 M $V_2(SO_4)_3$ + 2.75 M H_2SO_4, respectively, which were prepared by electrolyzing 1 M $VOSO_4$ + 3 M H_2SO_4 solution. When evaluating the negative redox couple, N_2 was purged into the electrolyte to form an inert atmosphere, avoiding the chemical oxidation of V^{2+} to V^{3+}.

2.3. Single cell assembly

Two methods were designed for applying CCM in VFB, as shown in Fig. 1. One was using CCM (WO_3/SAC loading 1 mg cm^{-2}) to replace the membrane of traditional cell structure. Thus, the electrode was still the graphite felt. The utilization of CCM means that the catalyst layer is introduced between the electrode and the membrane. Compared with the traditional structure, the mass and volume were almost unchanged. Another method was directly assembling the cell with current collector and CCM (WO_3/SAC loading 3 mg cm^{-2}), eliminating the graphite felt electrode and the frame. The electrolyte flow field was carved on the surface of graphite plate current collector. The mass and volume of the battery were reduced significantly. Constant current charge–discharge tests were carried out on a battery test system Arbin-010 MITS pro 4.0-BT2000 instrument (Arbin Co., USA). For contrast, the traditional structure flow cell was assembled employing graphite felt (3 cm × 3 cm in area, the thickness before and after the cell assembly was 6 and 4 mm, respectively, the compression ratio was 66.67%) as electrode, Nafion115 membrane (Dupont Inc., USA, 5 cm × 5 cm) as the separator and graphite plate (2 mm in thickness) as the current collector. The cell cavity was around 12 mm [2 mm (positive collector) + 4 mm (positive electrode) + 4 mm (negative electrode) + 2 mm (negative collector), neglecting the thickness of the membrane]. The initial positive and negative electrolytes were 30 mL 1.5 M $VOSO_4$ + 3 M H_2SO_4 and 30 mL 0.75 M $V_2(SO_4)_3$ + 2.25 M H_2SO_4, respectively, stored in the outside tanks and pumped into the compartments when the flow cell

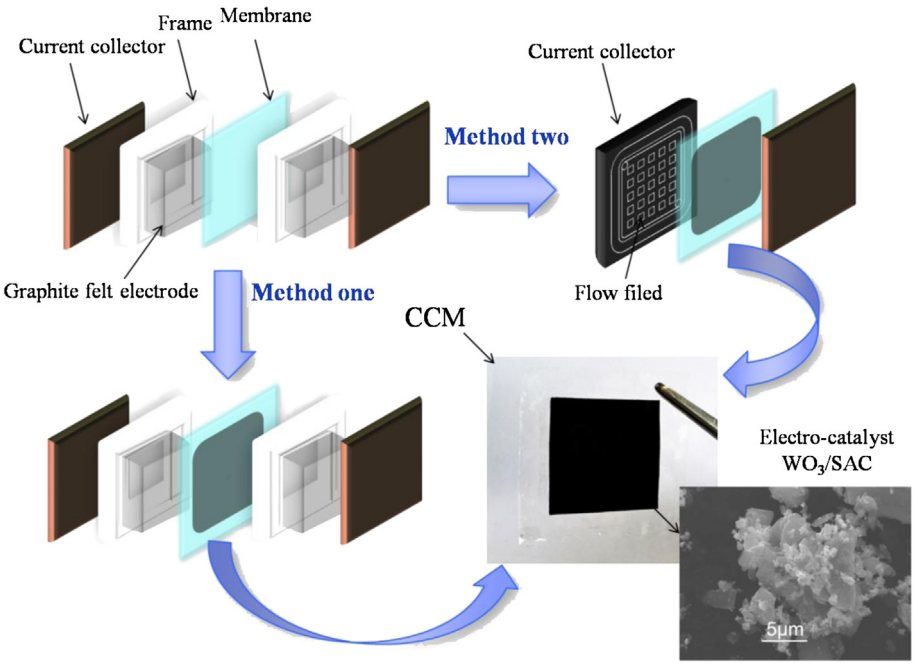

Fig. 1. Sketch map of the single cell assembly basing on CCM architecture.

dynamic running. The cell coulombic efficiency (CE) was defined as the discharge capacity divided by the charge capacity, while the energy efficiency (EE) was defined as the discharge energy divided by the charge energy. Then the voltage efficiency (VE) can be calculated from the equation VE = EE/CE [25].

2.4. AC electrochemical impedance investigation

To further understand the effect of CCM on electrode processes, a straightforward technique is to measure the change in the electrical impedance of electrochemical device by an AC impedance method. In this study, AC impedance determinations were carried out on single cells under constant current work state on Arbin-010 MITS pro 4.0-BT2000 workstation. The charge and discharge current density was 120 mA cm^{-2}, and the high charge voltage limit and the low discharge voltage limit were set at 1.65 V and 1.0V, respectively. A sine current wave I, the amplitude of which was 50 mA at frequency 1 kHz (6283.2 rad s^{-1}), was applied to the device. The potential response V and the phase shift θ between current and voltage were measured by the device. The resulting data can be used to calculate the AC impedance Z_0, the magnitude of the ratio of the voltage and current waveforms.

3. Results and discussion

3.1. Electrochemical performance comparison of graphite felt and electro-catalyst WO_3/SAC

The electrochemical performances of electro-catalyst WO_3/SAC and the graphite powder are shown in Fig. 2. The sweep voltage windows were set at −0.7 to −0.2 V and 0.5–1.1 V vs. SCE for V^{2+}/V^{3+} and VO^{2+}/VO_2^+ redox couples, respectively. In these ranges, the oxidation and reduction peaks are all detected on the two electrodes; however, the shapes are different. It can be seen clearly from Fig. 2(a) that, compared with the graphite powder electrode, the peak currents of the redox reaction are much higher and the peak potential gap is smaller on the electro-catalyst WO_3/SAC electrode. Besides, the onset potentials of the oxidation process on the WO_3/SAC electrode and graphite powder electrode are 0.74 V and 0.87 V, respectively, which means that the VO^{2+} can be oxidized to VO_2^+ more easily on the former electrode [17]. The similar results can be found for the negative redox couple in Fig. 2(b). Fig. 3 shows the CV curves under different scanning rates. With increasing scan rate, the peak currents of electro-catalyst WO_3/SAC electrode are enhanced obviously, whereas the peak potential gap encounters no change,

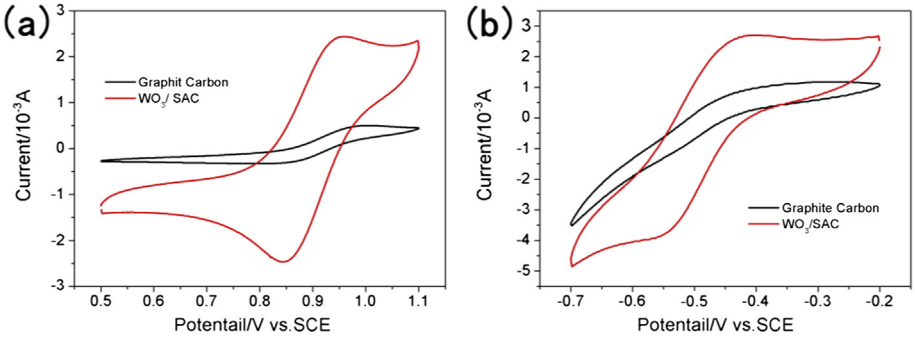

Fig. 2. CV curves of graphite powder electrode and electro-catalyst WO_3/SAC electrode at a scan rate of 10 mV s^{-1} in positive electrolyte 0.5 M $VOSO_4$ + 0.25 M $(VO_2)_2SO_4$ + 3.25 M H_2SO_4 (a) and in negative electrolyte 0.5 M VSO_4 + 0.25 M $V_2(SO_4)_3$ + 2.75 M H_2SO_4 (b).

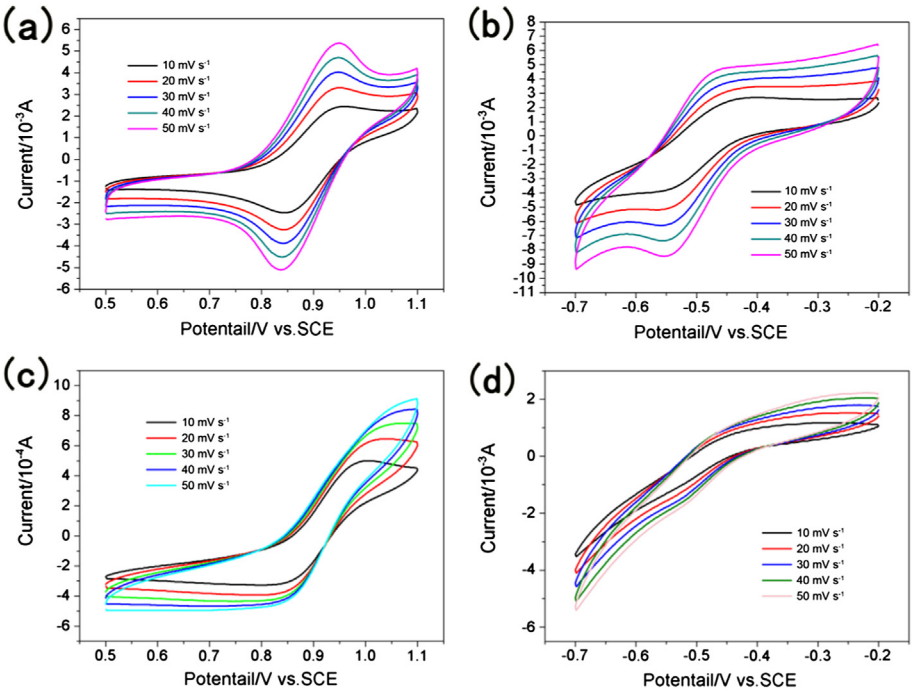

Fig. 3. CV curves of electro-catalyst WO_3/SAC electrode in 0.5 M $VOSO_4$ + 0.25 M $(VO_2)_2SO_4$ + 3.25 M H_2SO_4 (a) and in 0.5 M VSO_4 + 0.25 M $V_2(SO_4)_3$ + 2.75 M H_2SO_4 (b) and graphite powder electrode in 0.5 M $VOSO_4$ + 0.25 M $(VO_2)_2SO_4$ + 3.25 M H_2SO_4 (c) and in 0.5 M VSO_4 + 0.25 M $V_2(SO_4)_3$ + 2.75 M H_2SO_4 (d) under different scanning rates.

indicating that the VO^{2+}/VO_2^+ and V^{2+}/V^{3+} redox reactions are quite reversible on this electrode. By contrast, the shapes of redox peaks using graphite carbon electrode are not as symmetrical as that using electro-catalyst WO_3/SAC electrode, and the peak potential gap becomes larger when the scan rate increases, denoting that the reversibility is inferior to the electro-catalyst WO_3/SAC electrode. Fig. 4 presents the morphologies of the two materials. Compared with the graphite powder, SAC provides larger surface area and the WO_3 particles introduce more active centers for redox reactions. The catalytic mechanism of WO_3/SAC has been discussed in Ref. [24]. Therefore, the electro-catalyst WO_3/SAC exhibits much favorable electrochemical activity and kinetic reversibility toward V(IV)/V(V) and V(II)/V(III) redox couples than that of the graphite powder electrode.

100 Cycles repeating sweeping measurements were carried out to identify the durability of the electro-catalyst WO_3/SAC. The

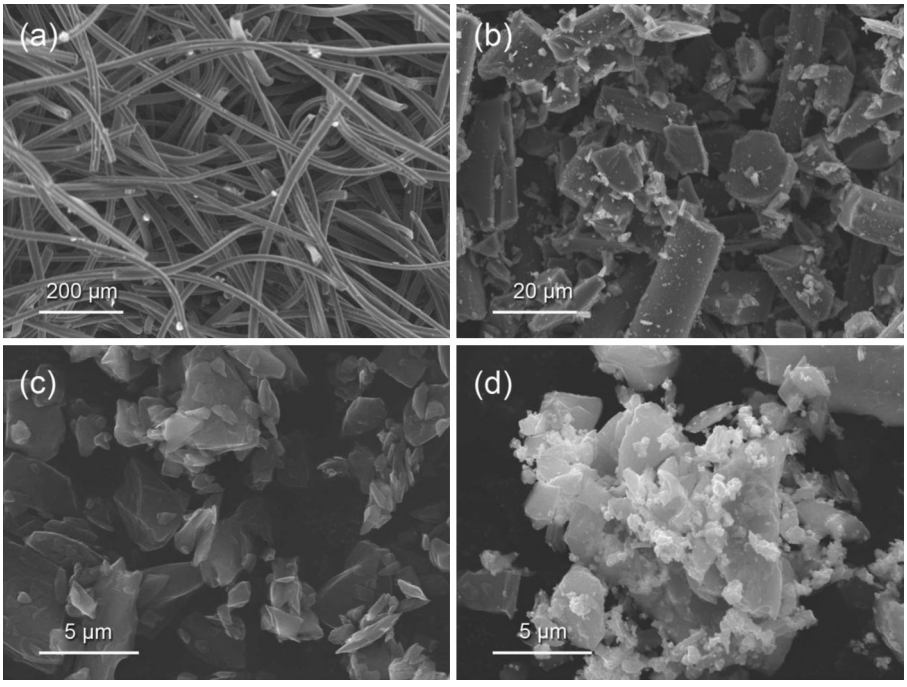

Fig. 4. Morphology of graphite felt (a), graphite powder (b), SAC (c) and electro-catalyst WO_3/SAC.

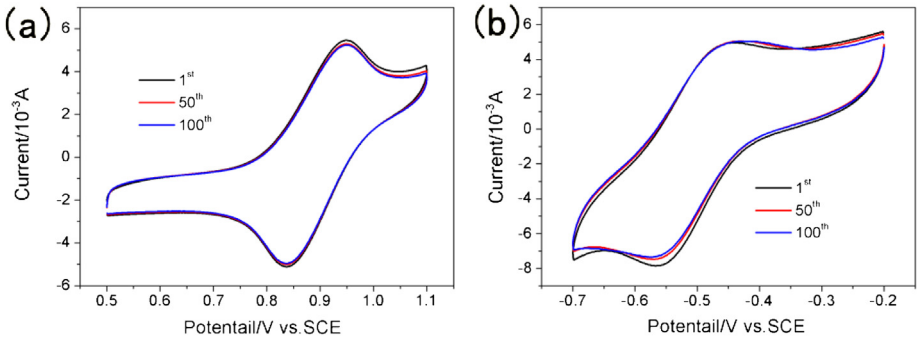

Fig. 5. 100 Cycles cyclic voltammetry curves of electro-catalyst WO_3/SAC electrode in 0.5 M $VOSO_4$ + 0.25 M $(VO_2)_2SO_4$ + 3.25 M H_2SO_4 (a) and in 0.5 M VSO_4 + 0.25 M $V_2(SO_4)_3$ + 2.75 M H_2SO_4 (b) with a sweep rate 50 mV s^{-1}.

profiles of the 1st, 50th and 100th cycles are shown in Fig. 5. Comparing the 50th cycle with the 1st cycle, the redox peak currents and the peak potential gap change a little. The profiles of the 50th and 100th cycle are almost identical. These results suggest that the electro-catalyst WO_3/SAC electrode has durable catalytic performance for both VO^{2+}/VO_2^+ and V^{2+}/V^{3+} redox couples. The catalyst layer prepared by spraying catalyst ink on membrane (CCM) is very similar to that by dropping catalyst ink on the glass carbon dick electrode. Hence, it can be presumed that CCM could exhibit an enhanced electrochemical performance, which will help to accelerate electrode reactions kinetics and improve the energy conversion efficiency when it is applied to VFB.

3.2. Single cell performance based on CCM architecture

For CCM application, two methods were designed as described above and the charge–discharge experiments were performed accordingly. Fig. 6 presents the charge–discharge curves of the cell assembled by the first method at different current densities, compared with the traditional structure single cell. It can be seen from the figure that the cell assembled with graphite felt + CCM possesses lower charge voltage plateau and higher discharge voltage plateau than the cell assembled with graphite felt + Nafion115. CCM architecture flow cell also has longer charge time, which means that a higher charge capacity is obtained. The detailed efficiency data were listed in Table 1. The coulombic efficiency (CE), voltage efficiency (VE) and energy efficiency (EE) of CCM architecture single cell are 94.6%, 85.9% and 81.2%, respectively, at a current density of 120 mA cm^{-2}. The VE and EE are much higher than that of traditional structure single cell, 81.3% and 76.9%, respectively. The improvement can be attributed to the usage of CCM, on which the electro-catalyst layer has accelerated the progress of electrode reactions. You et al. reported a two-dimensional stationary mode to describe a single vanadium flow cell based on the universal conservation laws and coupled with electrochemical reactions [26]. According to the result, the electrode reaction over-potential closed to the membrane side is relatively large. The introduction of electro-catalyst layer on the surface of membrane could reduce the over-potential, due to the excellent electrochemical activity and kinetic reversibility. Fig. 7 provides the

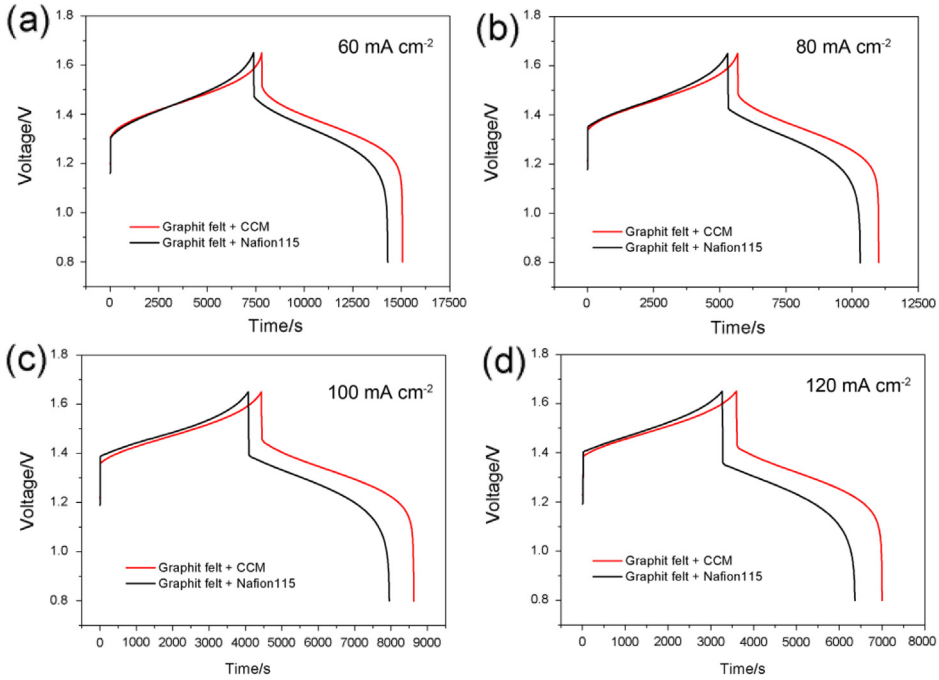

Fig. 6. Charge–discharge profiles comparison of the cell assembled with conversional graphite felt + Nafion115 and the cell assembled with graphite felt + CCM at 60 mA cm^{-2} (a), 80 mA cm^{-2} (b), 100 mA cm^{-2} (c), and 120 mA cm^{-2} (d).

Table 1
Efficiencies of the cells assembled with graphite felt + Nafion115 and graphite felt + CCM (denoted as A and B, respectively), at current densities of 60, 80, 100 and 120 mA cm^{-2}.

Current density (mA cm^{-2})	Charge capacity (mA h)[a]		Disharge capacity (mA h)		Coulombic efficiency (%)		Voltage efficiency (%)		Energy efficiency (%)	
	A	B	A	B	A	B	A	B	A	B
60	1107.6	1180.6	1034.9	1092.1	93.4	92.5	90.1	92.5	84.1	85.6
80	1058.3	1133.4	1000.0	1064.9	94.4	93.9	86.7	90.1	82.0	84.7
100	1017.5	1106.7	966.4	1045.1	94.9	94.4	83.9	88.1	79.7	83.2
120	978.2	1078.5	925.7	1019.4	94.6	94.5	81.3	85.9	76.9	81.2

[a] The charge capacity at 100% SOC: 1206.25 mA h.

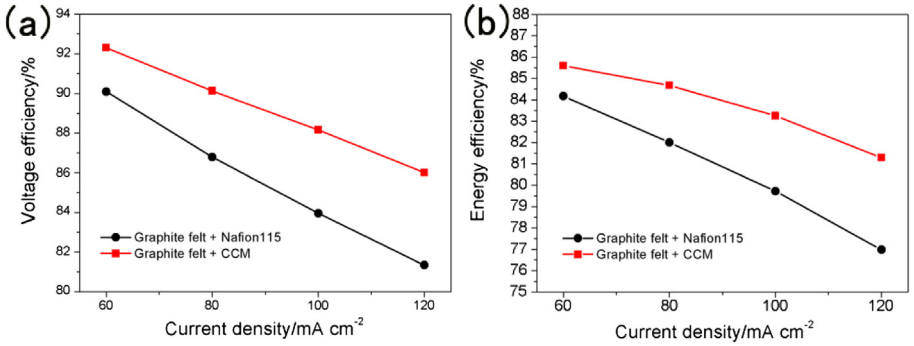

Fig. 7. The plots of voltage efficiency–current density (a) and energy efficiency–current density (b) for the cells assembled with graphite felt + Nafion115 and graphite felt + CCM.

plots of the voltage and energy efficiency as a function of current density. Energy efficiency and voltage efficiency are reduced with the increase of current density for the two cells; however, the decreasing rate is much slower for CCM architecture cell. With the increasing current density, the polarization and the charge transfer impedance of electrode reactions are increased, so the depolarizing effect provided by CCM becomes more obvious. Therefore, CCM structure is much propitious to charge–discharge in higher current density. Fig. 8 provides the life test results of the cell assembled with graphite felt + CCM at 120 mA cm^{-2}. The energy efficiencies keep higher than 80% during 300 cycles, and no degradation trend is observed, suggesting the favorable cycle stability of CCM.

Typical charge–discharge curves of the cell assembled using the second method are presented in Fig. 9. It can be found that the cell maintains good charge–discharge performance at lower current

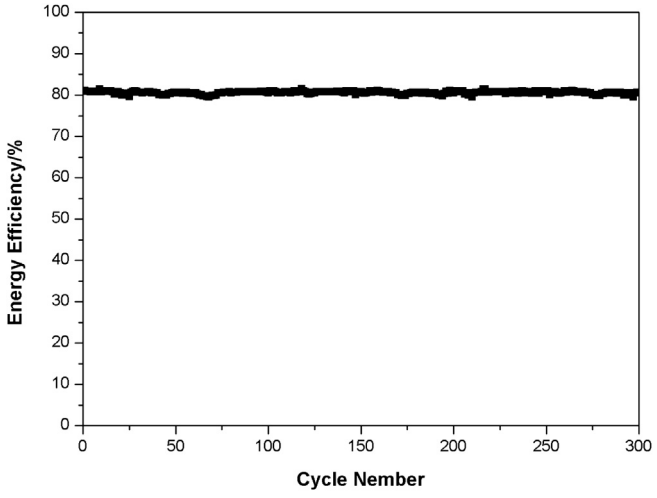

Fig. 8. Life test of the cell assembled by graphite felt + CCM at 120 mA cm^{-2}.

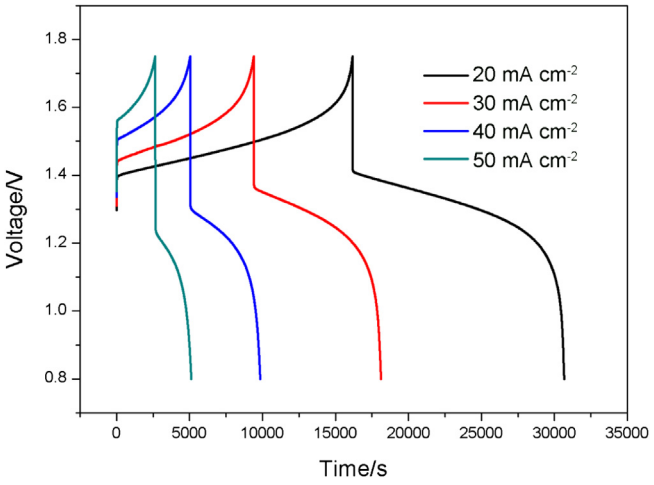

Fig. 9. Charge–discharge profiles of the cell directly assembled with current collector and CCM, at different current densities.

density. The efficiencies of the cell are listed in Table 2. At 20 mA cm^{-2}, the CE, VE and EE are 89.7%, 86.7% and 77.8%, respectively. Due to the elimination of the graphite felt electrode and frame, the mass and volume of the cell are reduced

Table 2
Efficiencies of the cell directly assembled with current collector and CCM, at current densities of 50, 40, 30 and 20 mA cm^{-2}.

Current density (mA cm^{-2})	Coulombic efficiency (%)	Voltage efficiency (%)	Energy efficiency (%)
50	95.2	68.6	65.3
40	94.0	75.3	70.8
30	92.3	81.4	75.1
20	89.7	86.7	77.8

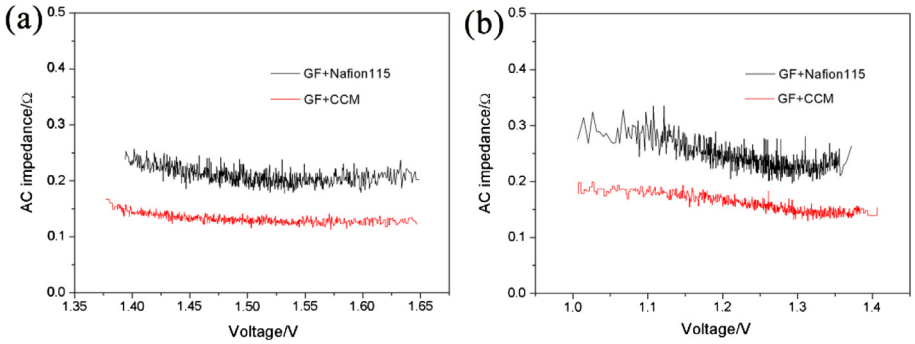

Fig. 10. AC impedance of the cells assembled with graphite felt + Nafion115 and graphite felt + CCM during charge (a) and discharge (b) processes at 120 mA cm^{-2}.

significantly, which helps to improve the energy density of VFB. However, at higher current density, the charge capacity and the efficiency are relatively low, since the active area is decreased and electrode reaction polarization is serious when eliminating the graphite felt. The present work is a primary experiment, and the further studies are necessary to improve the performance by way of optimizing the electro-catalyst and the flow field.

3.3. Electrochemical impedance spectroscopy analysis

Fig. 10 displays the AC impedance of the cells assembled with graphite felt + Nafion115 and graphite felt + CCM during the charge and the discharge processes at 120 mA cm^{-2}. It can be seen clearly that both in the process of charge and discharge, AC impedance Z_0 of the cell assembled with graphite felt + CCM is lower than that of the cell assembled with graphite felt + Nafion115. Z_0 is actually a complex parameter, which integrates the ohm resistance, charge transfer resistance and matter transfer resistance. For the two cells, key materials including electrode, electrolyte, membrane and current collector are the same, whereas, the only difference is derived from the electro-catalyst layer on membrane surface. The decrease of Z_0 should mainly attribute to the reduction of the charge transfer resistance since the electro-catalyst layer has provided highly active reaction sites and accelerated the kinetic process of electrode reactions. This result is consistent with the CV and the single cell performance.

4. Conclusions

CCM is a feasible way for electro-catalyst practical application in VFB. Using CCM to replace the membrane of traditional cell structure, the efficiencies and the power density of the flow cell are improved remarkably. The voltage efficiency and energy efficiency reach as high as 85.9% and 81.2% at 120 mA cm^{-2}, much higher than that of the traditional cell structure, 81.3% and 76.9%, respectively. The improvement can be attributed to that the accelerated electrode reactions and reduced charge transfer impedance by using electro-catalyst. The energy efficiencies keep higher than 80% during 300 cycles, suggesting a good stability of the CCM structure. Thus, CCM can be a promising cell structure for VFB with enhanced energy efficiency and power density.

Acknowledgments

This work is financially supported by National Basic Research Program of China (No. 2010CB227203).

References

[1] L. Joerissen, J. Garche, C. Fabjan, G. Tomazic, J. Power Sources 127 (2004) 98–104.
[2] M. Skyllas-Kazacos, M. Rychcik, R.G. Robins, A.G. Fane, J. Electrochem. Soc. 133 (1986) 1057–1058.
[3] I. Tsuda, K. Nozaki, K. Sakuta, K. Kurokawa, Sol. Energy Mater. Sol. Cells 47 (1997) 101–107.
[4] C. Poncede de León, A. Frías-Ferrer, J. González-García, D.A. Szánto, F.C. Walsh, J. Power Sources 160 (2006) 716–732.
[5] F. Rahman, M. Skyllas-Kazacos, J. Power Sources 189 (2009) 1212–1219.
[6] M. Skyllas-Kazacos, M.H. Chakrabarti, S.A. Hajimolana, F.S. Mjalli, M. Saleem, J. Electrochem. Soc. 158 (2011) R55–R79.
[7] M. Rychcik, M. Skyllas-Kazacos, J. Power Sources 19 (1987) 45–54.
[8] H. Kaneko, K. Nozaki, Y. Wada, T. Aoki, A. Negishi, M. Kamimoto, Electrochim. Acta 36 (1991) 1191–1196.
[9] X.G. Li, K.L. Huang, S.Q. Liu, N. Tan, L.Q. Chen, Trans. Nonferrous Met. Soc. China 17 (2007) 195–199.
[10] B.T. Sun, M. Skyllas-Kazacos, Electrochim. Acta 37 (1992) 1253–1260.
[11] B.T. Sun, M. Skyllas-Kazacos, Electrochim. Acta 37 (1992) 2459–2465.
[12] W.G. Zhang, J.Y. Xi, Z.H. Li, H.P. Zhou, L. Liu, Z.H. Wu, X.P. Qiu, Electrochim. Acta 89 (2013) 429–435.
[13] W.H. Wang, X.D. Wang, Electrochim. Acta 52 (2007) 6755–6762.
[14] Z. González, A. Sánchez, C. Blanco, M. Granda, R. Menéndez, R. Santamaría, Electrochem. Commun. 13 (2011) 1379–1382.
[15] C. Flox, J. Rubio-Garcia, R. Nafria, R. Zamani, M. Skoumal, T. Andreu, J. Arbiol, A. Cabot, J.R. Morante, Carbon 50 (2012) 2347–2374.
[16] K.J. Kim, M.S. Park, J.H. Kim, U. Hwang, N.J. Lee, G.J. Jeong, Y.J. Kim, Chem. Commun. 48 (2012) 5455–5457.
[17] W.Y. Li, J.G. Liu, C.W. Yan, Carbon 49 (2011) 3463–3470.
[18] Y.Y. Shao, X.Q. Wang, M. Engelhard, C.M. Wang, S. Dai, J. Liu, Z.G. Yang, Y.H. Lin, J. Power Sources 195 (2010) 4375–4379.
[19] P.X. Han, H.B. Wang, Z.H. Liu, X. Chen, W. Ma, J.H. Yao, Y.W. Zhu, G.L. Cui, Carbon 49 (2011) 693–700.
[20] R.L. Jia, S.M. Dong, T. Hasegawa, J.P. Ye, R.H. Dauskardt, Int. J. Hydrogen Energy 37 (2012) 6790–6797.
[21] I.S. Park, W. Li, A. Manthiram, J. Power Sources 195 (2010) 7078–7082.
[22] H.L. Tang, S.L. Wang, M. Pan, S.P. Jiang, Y.Z. Ruan, Electrochim. Acta 52 (2007) 3714–3718.
[23] P. Trogadas, E. Pinot, T.F. Fuller, Electrochem. Solid-State Lett. 15 (2012) A5–A8.
[24] C. Yao, H.M. Zhang, T. Liu, X.F. Li, Z.H. Liu, J. Power Sources 218 (2012) 455–461.
[25] P. Qian, H.M. Zhang, J. Chen, Y.H. Wen, Q.T. Luo, Z.H. Liu, D.J. You, B.L. Yi, J. Power Sources 175 (2008) 613–620.
[26] D.J. You, H.M. Zhang, J. Chen, Electrochim. Acta 54 (2009) 6827–6836.